# SCIENCE AND TECHNOLOGY

Srđan BOŠNJAK
Miodrag ARSIĆ
Sreten SAVIĆEVIĆ
Goran MILOJEVIĆ
Dušan ARSIĆ

## FRACTURE ANALYSIS OF THE PULLEY OF A BUCKET WHEEL BOOM HOIST SYSTEM

## ANALIZA PĘKNIĘĆ KOŁA PASOWEGO UKŁADU WCIĄGARKI WYSIĘGNIKA KOŁA CZERPAKOWEGO

*This paper presents the results of the pulley fracture analysis. Experimental investigations confirmed that the chemical composition and basic mechanical properties of the pulley material, except the impact energy at a temperature of –20°C, meet the requirements of the corresponding standard. The impact energy value at the temperature of –20°C is for ≈45% lower than the prescribed value which has considerable influence on the appearance of the brittle fracture, especially having in mind the fact that the bucket wheel excavators operate at low temperatures. Metallographic examinations as well as magnetic particle inspections indicated that initial cracks in the welded joints occurred during the manufacture of the pulleys. Characteristic levels of the rope load cycle are obtained by using in-house software which includes the dynamic effects of the resistance-to-excavation. The FEA results pointed out that in the representative load cases the combinations of the mean stress and the alternating stress in the pulley critical zone lie considerably below the limit line of the modified Goodman's diagram. The conclusion, based on the presented results, is that the fracture of the pulley appeared as the result of the 'manufacturing-in' defects.*

*Keywords: bucket wheel excavator, pulley fracture, experimental investigations, FE stress analyses.*

*Artykuł przedstawia wyniki analizy pęknięć koła pasowego. Badania doświadczalne potwierdziły, że skład chemiczny oraz podstawowe właściwości mechaniczne materiału, z którego zostało wykonane koło pasowe, za wyjątkiem energii udaru w temperaturze –20°C, były zgodne z odpowiednią normą. Wartość energii udaru w temperaturze –20°C była o ≈45% niższa od wartości zalecanej, co ma znaczący wpływ na występowanie pękania kruchego, zwłaszcza gdy weźmie się pod uwagę fakt, że koparki kołowe są przeznaczone do pracy w niskich temperaturach. Badania metalograficzne oraz badania magnetyczno-proszkowe wykazały, że pęknięcie pierwotne w połączeniu spawanym pojawiło się już w fazie produkcji koła pasowego. Charakterystyczne poziomy cyklu obciążenia liny uzyskano stosując własne oprogramowanie, które uwzględnia dynamiczne oddziaływanie odporności na urabianie. Wyniki MES pokazały, że w przypadku obciążeń reprezentatywnych, wartości średniego naprężenia w funkcji naprężenia zmiennego w strefie krytycznej koła pasowego były znacznie niższe niż wartości graniczne wyznaczone na podstawie zmodyfikowanego wykresu Goodmana. Na podstawie otrzymanych wyników stwierdzono, że pęknięcie koła pasowego powstało wskutek wad produkcyjnych.*

*Słowa kluczowe: koparka kołowa, pęknięcie koła pasowego, badania doświadczalne, analiza naprężeń metodą elementów skończonych.*

## 1. Introduction

The bucket wheel boom (BWB) of the bucket wheel excavator (BWE) SRs 1300 (Fig. 1) is hung by two stays hinged to the trolley with the pulley block (the so-called "moving pulley block"). Changing of the BWB inclination angle is realized by shifting the moving pulley block.

The BWB hoist system is the vital part of the BWE. Failures of its components may lead to catastrophic consequences as described in [1, 3, 34]. Even in cases where the direct failure effects are not so drastic, the indirect financial losses are high [9, 10, 13]. In-service fracture of one pulley of the fixed pulley block (Fig. 2) is a typical example of a failure in which the direct material loss (≈3,000 €) is far less than the indirect financial loss (714,000 €) caused by the system downtime during the execution of very complex operations such as: temporary
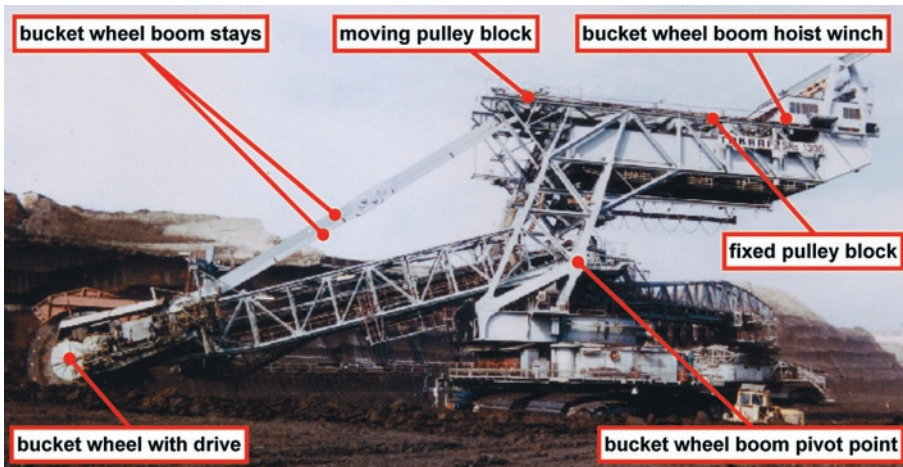
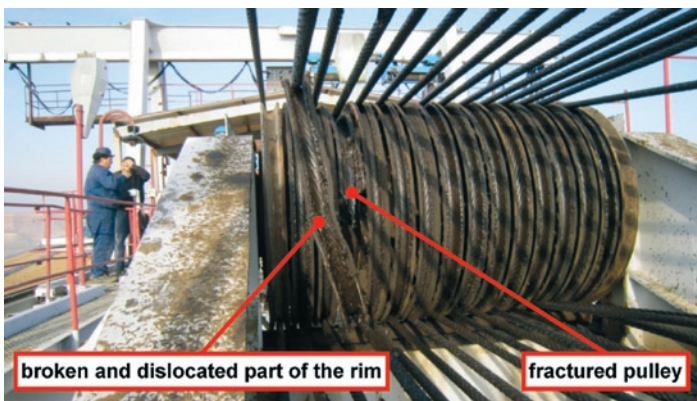*Fig. 1. BWE SRs 1300: total weight 2303 t; theoretical capacity 4500 m³/h*



*Fig. 2. Fracture of the pulley of the fixed pulley bloc*
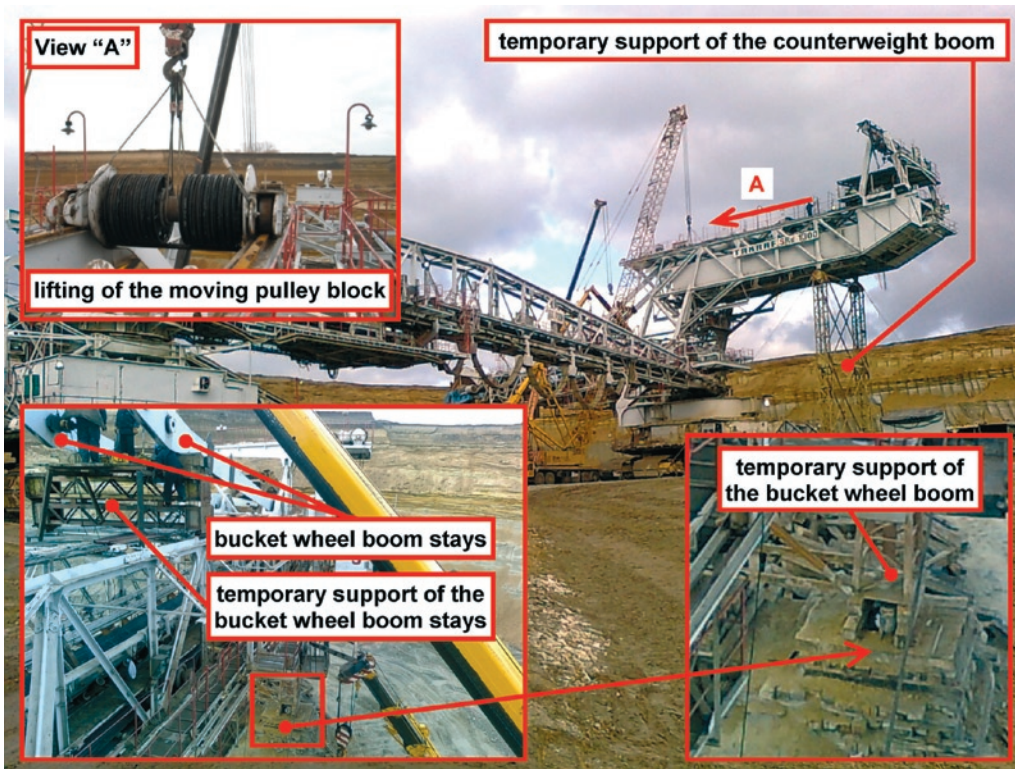


*Fig. 3. Details of the BWE temporary supports and the dismantling of the BWB hoist system*

supporting of the machine, dismantling of the BWB hoist system, testing and repair of the failed pulleys, testing of the rope and reassembling the BWB hoist system (Fig. 3, Table 1).

The goals of the study presented in the paper were to: (1) Develop a method of identifying pulley working loads, taking into account the dynamic nature of the external loads caused by the resistance-to-excavation; (2) Establish the procedure and determine the cause of pulley fracture; (3); To give the expert judgment: repair or redesign the pulleys.

The following sections will present details of the carried out experimental and numerical researches and the conclusions arrived at therein. The investigation results are important because: (a) pulleys are vital parts of the rope mechanisms; (b) same or similar problems could arise in rope hoisting mechanisms of not only various types of mining machines [40] but also of a wide class of construction machines and cranes. Besides, research results indicate the importance of the non-destructive testing (NDT) of welded joints of the BWE vital structural parts.

Table 1. Specification of costs due to the overburden system downtime caused by one pulley failure

| Nomenclature | Cost in € |
|---|---|
| DT and NDT testing before, during and after the pulley repair | 6,000 |
| Engagement of workers and machines | 36,000 |
| 14–days system downtime (14 x 24 h x 2,000 €/h) | 672,000 |
| Total | 714,000 |

## 2. Fracture description

During BWE exploitation a failure of the welded joints of the spokes and rim occurred, which led to the plastic deformation and fracture of the rim (Figs 4a, b). Apart from that, plastic deformations of the spokes are observed (Fig. 4c) as well as fractures of their welded joints with the hub.

## 3. Experimental investigations

### 3.1. Destructive testing

According to the design documentation, the pulleys were supposed to be made from steel quality grade St 37-3 (according to the code [11]). Experimental examinations are performed on samples taken from the damaged pulley (Fig. 5). Results of the chemical analysis, tensile and impact tests are presented in Tables 2–4. Average macro-hardness is 129 HB [17].

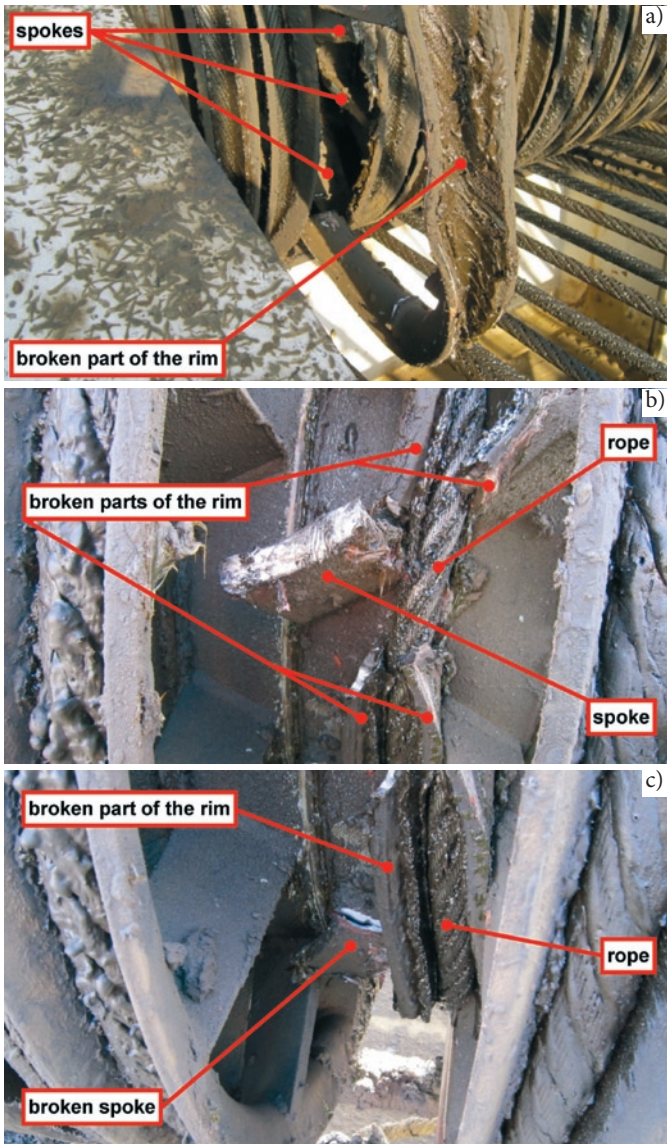Metallographic examinations are carried out on the replicas [28]

Fig. 4. Details of the fractured pulley: (a) front view; (b) back view; (c) view from below
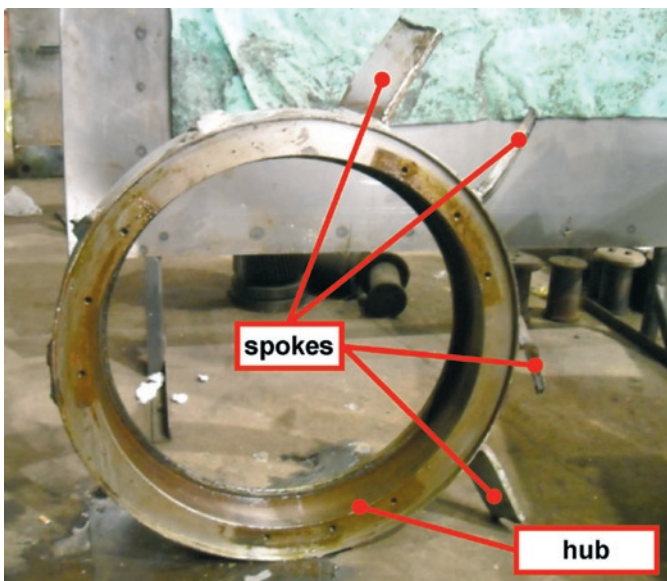


Fig. 5. A part of the damaged pulley used for sampling

Table 2. Chemical analysis (wt.%) of the pulley material and chemical composition of St 37-3 [11]

| Material | C | Si | Mn | S | P | Al |
|---|---|---|---|---|---|---|
| Sample | 0.159 | 0.188 | 0.625 | 0.018 | 0.016 | 0.004 |
| St 37-3 | max. 0.19 | – | – | max. 0.050 | max. 0.050 | – |

Table 3. Tension test [14] results of the pulley material and tensile properties of St 37-3 [11]

| Specimen | $\sigma_{YS}$ (MPa) | $\sigma_{UTS}$ (MPa) | Elongation $A_{50}$ (%) | Contraction Z (%) |
|---|---|---|---|---|
| 1 | 278 | 434 | 44.5 | 46.9 |
| 2 | 283 | 433 | 38.2 | 44.4 |
| 3 | 281 | 435 | 40.5 | 44.4 |
| St 37-3 | min. 235 | 360–510 | min. 24 | – |

Table 4. Impact energy test [15] results of the pulley material and impact energy of St 37-3 [11]

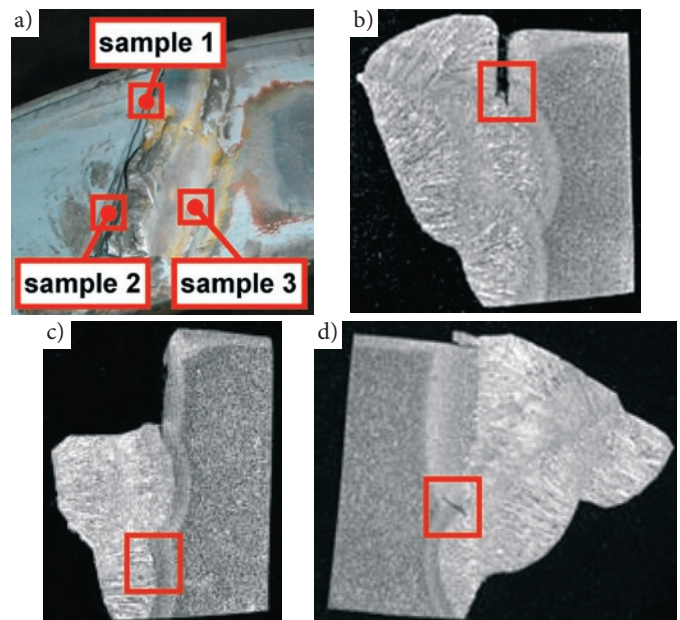| Temperature | Specimen | Impact energy $KV_{300/2}$ (J) | Average (J) |
|---|---|---|---|
| –20°C | 1 | 14.7 | 14.7 |
| | 2 | 12.7 | |
| | 3 | 16.7 | |
| | St 37-3 | min. 27 | – |
| 0°C | 4 | 39,2 | 40.5 |
| | 5 | 42.2 | |
| | 6 | 40.2 | |



Fig. 6. Sampling zones (a) and samples: 1 – (b), 2 – (c), 3 – (d)

taken from the welded joint of the spoke and hub (Fig. 6). Grain sizes were determined using the standard [19], and the content of the non-metallic inclusions according to the code [20] (Figs. 7, 8).

### 3.2. Non-destructive testing

After dismantling the fixed and moving pulley blocks (Fig. 3) the magnetic particle inspection (MPI) of the fillet welds was carried out according to the code [16]. Crack indications (Fig. 9, Table 5) were
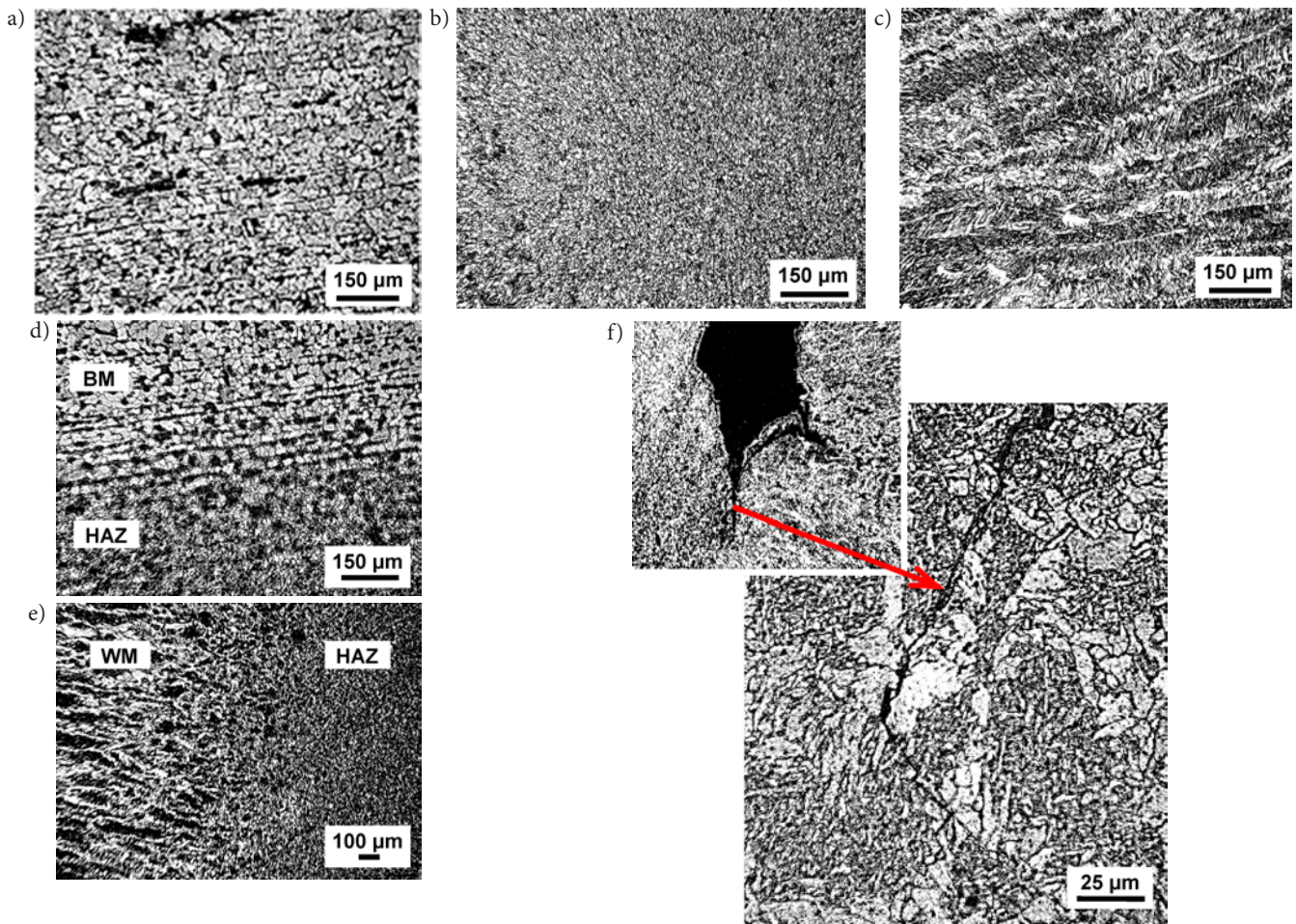
*Fig. 7. Sample 1 (etched with 3% nital): (a) strip-type ferrite-pearlite microstructure of the BM, microhardness of 140–144 HV1 [27]; (b) fine-grained fer-rite-pearlite microstructure in HAZ, microhardness of about 159 HV1; (c) casting dendritic microstructure of the WM, microhardness of 172–197 HV1; (d) microstructure on the verge of the BM and HAZ; (e) microstructure on the verge of the WM and HAZ; (f) tip of the crack (depth ≈4 mm, width ≈0.5 mm) and its propagation*
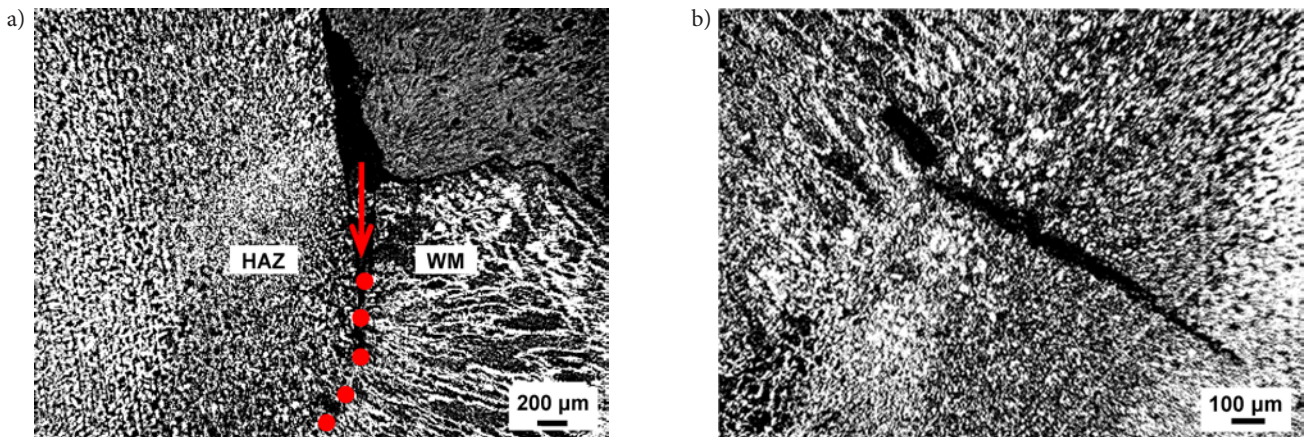


*Fig. 8. (a) Crack propagation alongside the verge of the WM and HAZ, sample 2 (framed detail in Fig. 6c); macrocrack (total length of ≈1.5 mm) initiated in WM and its propagation through HAZ and BM, sample 3 (framed detail in Fig. 6d)*

observed on all pulleys. They are considerably more pronounced on the welded joints of the spokes and rim than the welded joints of the spokes and hub.

## 4. Pulley stress analyses

The load analysis of the BWE structure is very complex due to its changeable geometry configuration (Fig. 10).

The forces in the rope of the BWB hoist system, shown in Fig. 11, are determined using standard [12]. The intensity of the cutting force is calculated based on the parameters of the BW drive, adopting [12] that the total cutting force is realized on one bucket only (Fig. 10). For load case (LC) H [12] the intensity of the cutting force ($U_{nom}$=298.5 kN) is calculated based on the nominal torque of the BW drive motor, whilst in LC HZ [12] its intensity ($U_{max}$=376.4 kN) is calculated based on the maximum torque of the clutch. In both LCs, rope force reaches its maximum for $\alpha_{BWB}$=3°15' (Fig. 11). It can be
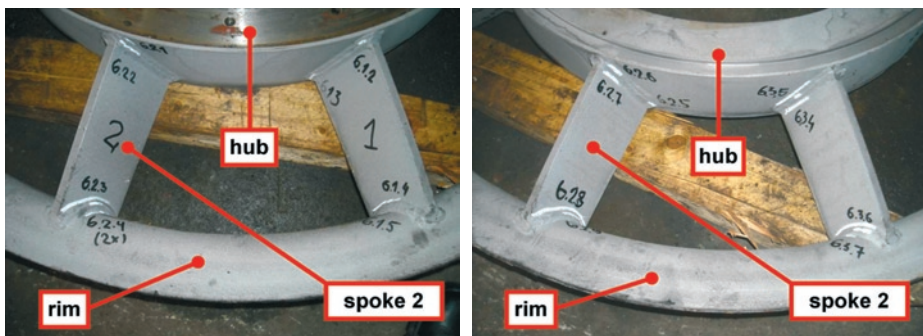
*Fig. 9. Typical MPI indications – pulley 6, spoke 2: (a) left side; (b) right side*

Table 5. *The MPI crack indications on spoke 2 (pulley 6).*

| Designation (a.b.c*) | 6.2.1 | 6.2.2 | 6.2.3 | 6.2.4 | 6.2.5 | 6.2.6 | 6.2.7 | 6.2.8 | 6.2.9 |
|---|---|---|---|---|---|---|---|---|---|
| Figure | 9a | | | | 9b | | | | |
| Length (mm) | 15 | 30 | 80 | 20;30 | 25 | 30 | 40 | 100 | 55 |

*\*a = ordinal of a pulley; b=ordinal of a spoke; c=ordinal of an indication.*

noted that usage of the procedure prescribed in [12] leads to the loss of one of the key properties of the BWEs' working process – the dynamic character of the external load caused by resistance-to-excavation [2, 4, 6–8, 22–24, 29, 30, 32, 33, 35–39]. By extracting the static influence of the cutting force from the curves shown in Fig. 11 and introducing its dynamic influence determined in the manner presented in [2, 4], a more realistic character of changing of the rope force during the excavation process is obtained (Fig. 12, Table 6).

The stress state analyses are done by applying the finite element method (FEM). The 3D model of the pulley and rope (Fig. 13) was discretized by 10-node tetrahedron elements in order to create the FEM model (317,066 nodes, 185,852 elements, Fig. 14). Calculations are carried out for the maximum value of the angle between the legs of the rope $\alpha_{R,max}=5°$ (Fig. 13b). Interaction between the
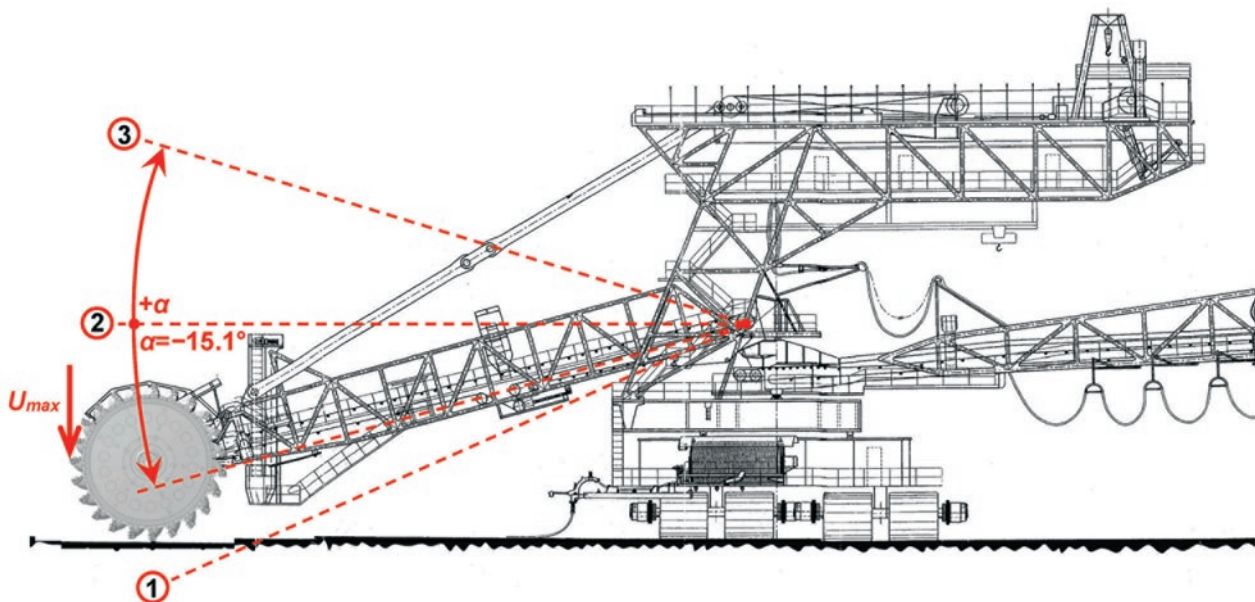


*Fig. 10. Characteristic BWB positions: 1 – low, $\alpha_{BWB}=-24°2'22''$; 2 – horizontal; 3 – high, $\alpha_{BWB}=16°34'48''$ (U–cutting force)*



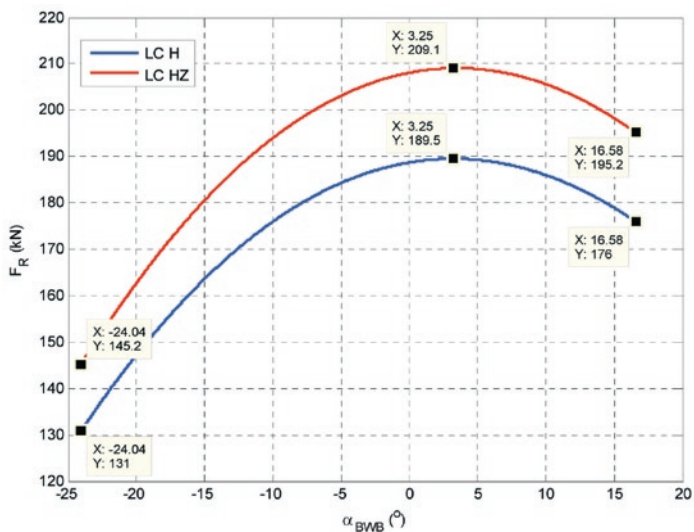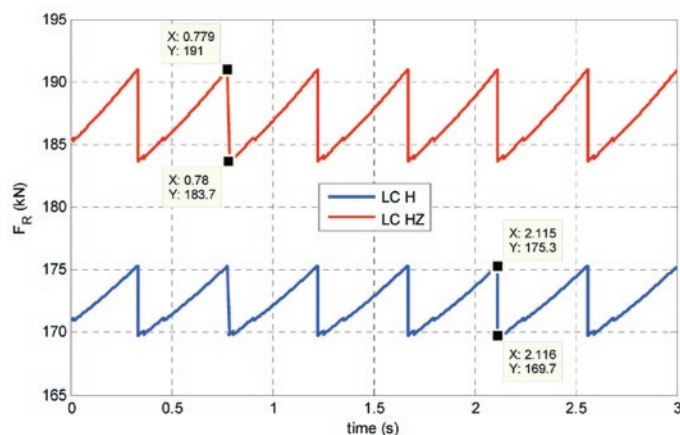*Fig. 11. The dependence of the rope force ($F_R$) on the BWB inclination angle ($\alpha_{BWB}$)*



*Fig. 12. Simulation of the rope force during the excavation process ($\alpha_{BWB}=3°15'$)*

Table 6. *Characteristic levels of the rope load cycle.*

| Load case | Rope force (kN) | | | |
|---|---|---|---|---|
| | maximum ($F_{Rmax}$) | minimum ($F_{Rmin}$) | mean ($F_{Rm}$) | amplitude ($F_{Ra}$) |
| H | 175.3 | 169.7 | 172.5 | 2.8 |
| HZ | 191.0 | 183.7 | 187.35 | 3.65 |

tained by using code [12], the maximum von Mises stress value in the T-fillet welded connection of the rim is $\sigma_{vM\,max,[12]} = 186$ MPa.

## 5. Discussion

In order to make a decision on whether to repair or redesign the pulleys, it was necessary to conduct a complex procedure whose basic stages are shown in Fig. 16.

In the considered case, both pulley design and the material were adequately selected – steel quality grade RSt 37-3 is commonly used for manufacturing the pulley blocks for the bucket wheel excavators. Based on the testing results presented in Tables 2–4 it is conclusive that the chemical composition and the basic mechanical properties of the pulley material, except the impact energy value at the temperature of –20℃, meet the requirements of standard [11] prescribed for steel grade RSt 37-3. Namely, the impact energy value at the temperature of –20℃ is for ≈45% lower (Table 4) than the value listed in [11] which has considerable influence on the appearance of the brittle fracture, especially having in mind the fact that the BWEs operate at low temperatures.

Micrographic testing indicates the notably structural heterogeneity of the welds. BM has the strip-type ferrite-pearlite microstructure with non-metallic inclusions of both oxide and sulfide type (Fig. 7a). The microstructure in HAZ (Fig. 7b) is fine-grained ferrite-pearlite with fine-grained oxide type non-metallic inclusions. WM has the casting dendritic microstructure (Fig. 7c) because the appropriate heat treatment of the pulley welded structure was not carried out. Under fatigue loading the non-metallic inclusions in BM and HAZ may cause the appearance of initial cracks, whilst the dendritic microstructure of the WM indicates the tendency towards the brittle fracture. Poor manufacturing practice led to multiple welding defects – incomplete welding (Fig. 6b). Those defects significantly accelerate premature crack initiation by playing a role, from the welding point of view, as the local HAZ based weak link.

The considerably more pronounced presence of the MPI crack indications at welded joints of the spokes and rim is the consequence of their geometry being more complex than the geometry of the welded joints of the spokes and hub.

In accordance with the recommendations [25, 26] regarding fatigue safety evaluation, it is adopted that the fatigue limit of the critical welded joint is $S_e$=45 MPa. The tensile strength of the weld metal ($\sigma_c$) is determined by the following expression [31]:
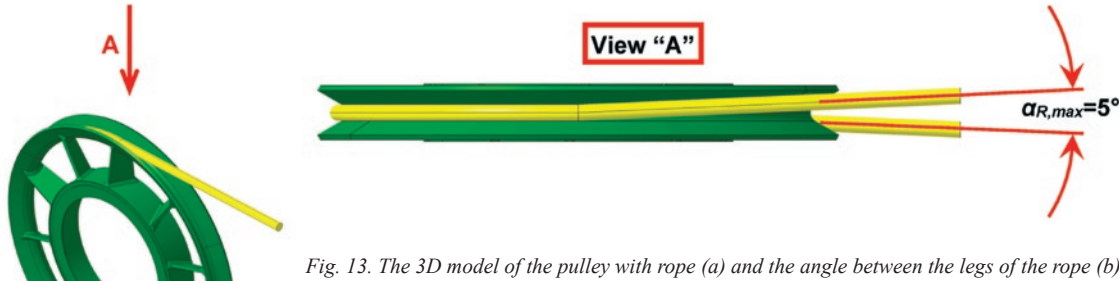


Fig. 13. *The 3D model of the pulley with rope (a) and the angle between the legs of the rope (b)*

rope and the pulley was simulated by contact connection. Maximum values of von Mises stresses are obtained in the T-fillet welded connections of the rim (Fig. 15). The characteristic stress levels of the pulley load cycle during excavation for both considered LCs are presented in Table 7. For the maximum rope force (209.1 kN, Fig. 11) ob-
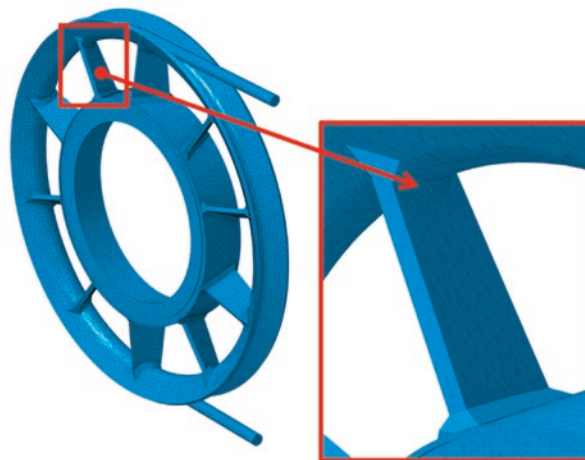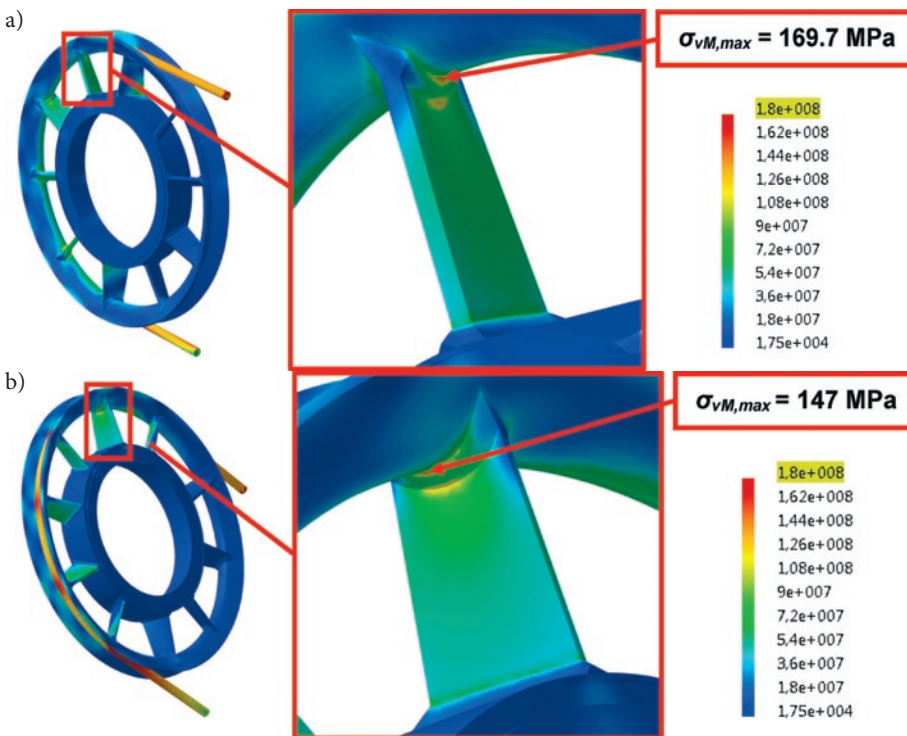


Fig. 14. *The FEM model*



Fig. 15. *The von Mises stress field obtained for $F_R$=191 kN (the maximum rope force in LC HZ, Fig. 12)*

Table 7. *Characteristic levels of the pulley stress cycle.*

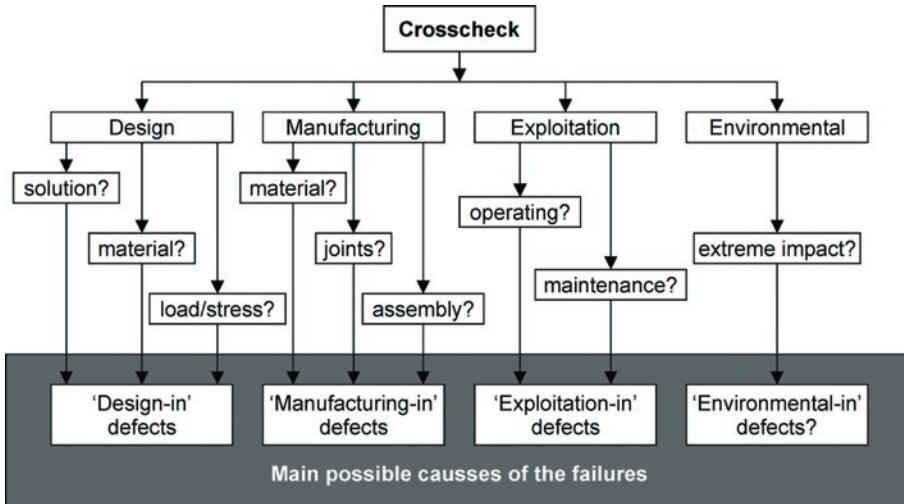| Load case | Stress value (MPa) | | | |
|---|---|---|---|---|
| | maximum ($\sigma_{max}$) | minimum ($\sigma_{min}$) | mean ($\sigma_m$) | amplitude ($\sigma_a$) |
| H | 155.8 | 150.8 | 153.3 | 2.5 |
| HZ | 169.7 | 163.3 | 166.5 | 3.2 |



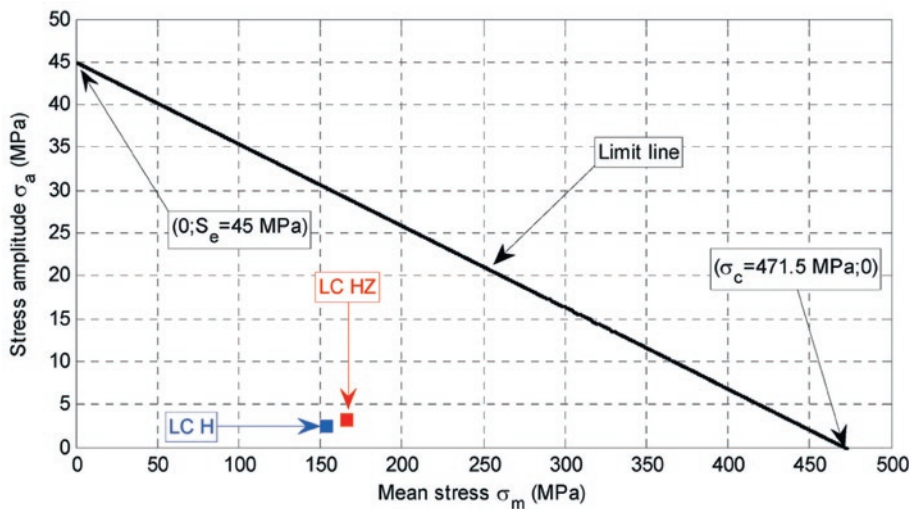Fig. 16. *The procedure of determining the causes of pulley fracture*



Fig. 17. *The modified Goodman diagram*

$$\sigma_c = 0.5\sigma_w + 0.5\sigma_{UTS\,min} = 0.5 \times 510 + 0.5 \times 433 = 471.5 \text{ MPa, (1)}$$

where $\sigma_w$=510 MPa is the ultimate tensile strength of deposited metal (electrode BÖHLER FOX EV 50 [18]), while $\sigma_{UTSmin}$=433 MPa is the minimum ultimate tensile strength value of base metal obtained by tensile testing (Table 3).

It is obvious (Fig. 17) that in both representative LCs the combinations of the mean stress and the alternating stress in the critical zone (Table 7) lie considerably below the limit line connecting the fatigue limit $S_e$ and the tensile strength of the weld metal $\sigma_c$. Besides that, in the case of the maximum rope force obtained by using code [12], the maximum von Mises stress value ($\sigma_{vM\,max,[12]}$) is 2.5 times lower than the tensile strength of the weld metal ($\sigma_c$, Eq. (1)).

Based on the presented results, it was concluded that the pulley fracture was caused by the 'manufacturing-in' defects. That is why it was decided to carry out the repairs of the pulley spokes' welded joints, without modifying their design.

## 6. Conclusion

Perennial exploitation of the BWEs in harsh working conditions leads to a gradual degradation of their subsystems. Despite rigorous controls during designing, manufacturing and assembling, compliant with the relevant standards, failure occurrence is almost inevitable during BWEs exploitation. Their causes could be of the different nature [5, 21] which is determined by using the procedure presented in Section 5.

Load analysis of the fractured pulley was carried out by using the original procedure which includes the dynamic effects of the resistance-to-excavation, unlike the procedure prescribed by code DIN 22261-2 [12]. Results of the FEAs indicate that the considered pulley is designed in full accordance with its function and working loads.

The considerably lower impact toughness at the temperature of −20°C points to the failures in the steelmaking technology. Metallographic examinations as well as MPIs indicate that the initial cracks in the welded joints occurred during the manufacture of the pulleys. Apart from that, the above mentioned cracks were located in the zones of maximum calculation stresses, which inevitably led to fracture. Therefore, the considered pulley fracture appeared as the result of 'manufacturing-in' defects [5, 21] which is why repairs of the spokes' welded joints of each of the pulleys were performed, without changing the design solution. This way, the downtime of the complete surface mining system, and indirect material losses were drastically reduced.

The presented investigation results underline the importance of the NDT of the vital structural parts' welded joints, both during production and the BWE's exploitation, especially in the zones of high calculated stress values. Finally, to the designers and manufacturers of the BWEs, the above mentioned investigation results present an indicator of the necessity to increase the extent of controls during the BWEs' manufacturing and assembling, prescribed by relevant standards, especially when it comes to the sub-systems whose failures can cause serious material and financial losses. Properly prescribed and conducted technical diagnostics is the basis of rational technical-economical, reliable and safe operation of the BWEs.

## References

1    Araujo LS, de Almeida LH, Batista EM, Landesmann A. Failure of a bucket-wheel stacker reclaimer: metallographic and structural analyses. Journal of Failure Analysis and Prevention 2012; 12: 402-407, http://dx.doi.org/10.1007/s11668-012-9575-z.

2.   Arsić M, Bošnjak S, Zrnić N, Sedmak A, Gnjatović N. Bucket wheel failure caused by residual stresses in welded joints. Engineering Failure Analysis 2011; 18(2): 700-712, http://dx.doi.org/10.1016/j.engfailanal.2010.11.009.

3.   Bošnjak S, Zrnić N, Simonović A, Momčilović D. Failure analysis of the end eye connection of the bucket wheel excavator portal tie-rod support. Engineering Failure Analysis 2009; 16(3): 740-750, http://dx.doi.org/10.1016/j.engfailanal.2008.06.006.

4.   Bošnjak S, Petković Z, Zrnić N, Simić G., Simonović A. Cracks, repair and reconstruction of bucket wheel excavator slewing platform. Engineering Failure Analysis 2009; 16(5): 1631-1642, http://dx.doi.org/10.1016/j.engfailanal.2008.11.009.

5.   Bošnjak S, Arsić M, Zrnić N, Rakin M, Pantelić M. Bucket wheel excavator: integrity assessment of the bucket wheel boom tie - rod welded joint. Engineering Failure Analysis 2011; 18(1): 212-222, http://dx.doi.org/10.1016/j.engfailanal.2010.09.001.

6.   Bošnjak S, Zrnić N. Dynamics, failures, redesigning and environmentally friendly technologies in surface mining systems. Archives of Civil and Mechanical Engineering 2012; 12(3): 348-359, http://dx.doi.org/10.1016/j.acme.2012.06.009.

7.   Bošnjak S, Oguamanam D, Zrnić N. The influence of constructive parameters on response of bucket wheel excavator superstructure in the out-of-resonance region. Archives of Civil and Mechanical Engineering 2015 (article in press); http://dx.doi.org/10.1016/j.acme.2015.03.009.

8.   Brkić A Đ, Maneski T, Ignjatović D, Jovančić P, Spasojević Brkić V K. Diagnostics of bucket wheel excavator discharge boom dynamic performance and its reconstruction. Eksploatacja i Niezawodnosc - Maintenance and Reliability 2014; 16 (2): 188-197.

9.   Bugaric U, Tanasijevic M, Polovina D, Ignjatovic D, Jovancic P. Lost production costs of the overburden excavation system caused by rubber belt failure. Eksploatacja i Niezawodnosc - Maintenance and Reliability 2012; 14 (4): 333-341.

10.  De Castro PMST, Fernandes AA. Methodologies for failure analysis: a critical survey. Materials & Design 2004; 25(2): 117-123, http://dx.doi.org/10.1016/j.matdes.2003.09.020.

11.  DIN 17100. Steels for general structural purposes. Deutsches Institut für Normung; 1980.

12.  DIN 22261-2. Bagger, Absetzer und Zusatsgeräte in Braunkohlentagebauen. Teil 2: Berechnungsgrundlagen. Deutsches Institut für Normung; 2006.

13.  Dreyer E. Cost-effective prevention of equipment failure in the mining industry. International Journal of Pressure Vessels and Piping 1995; 61(2-3): 329-347, http://dx.doi.org/10.1016/0308-0161(94)00114-X.

14.  EN 10002-1. Metallic materials - Tensile testing - Part 1: Method of test at ambient temperature. European Committee for Standardization; 1990.

15.  EN 10045-1. Mechanical testing of metals - Charpy impact test - Part 1: Test method. European Committee for Standardization; 1990.

16.  EN 1290. Non-destructive testing of welds - Magnetic particle testing of welds, European Committee for Standardization; 2004.

17.  EN ISO 6506-1. Metallic materials - Brinell hardness test - Part 1: Test method. European Committee for Standardization; 2005.

18.  EN ISO 2560. Welding consumables - Covered electrodes for manual metal arc welding of non-alloy and fine grain steels - Classification. European Committee for Standardization; 2009.

19.  EN ISO 643. Steels - Micrographic determination of the apparent grain size, European Committee for Standardization; 2012.

20.  EN 1024. Micrographic examination of the non-metallic inclusion content of steels using standard pictures, European Committee for Standardization; 2012.

21.  Gagg CR. Failure of components and products by 'engineered-in' defects: Case studies. Engineering Failure Analysis 2005; 12(6): 1000-1026, http://dx.doi.org/10.1016/j.engfailanal.2004.12.008.

22.  Golubović Z, Lekić Z, Jović S. Influence of bucket wheel vertical vibration on bucket-wheel excavator (BWE) digging force. Technical Gazette 2012; 19(4): 807-812.

23.  Gottvald J. The calculation and measurement of the natural frequencies of the bucket wheel excavator SchRs 1320/4x30. Transport 2010; 25(3): 269-277. http://dx.doi.org/10.3846/transport.2010.33

24.  Gottvald J. Analysis of vibrations of bucket wheel excavator SchRs 1320 during mining process. FME Transactions 2012; 40(4):165-170.

25.  Hobbacher AF. Recommendations for fatigue design of welded joints and components. IIW Document XIII-2151r3-07/XV-1254r3-07. International Institute of Welding; 2008.

26.  Hobbacher AF. The new IIW recommendations for fatigue assessment of welded joints and components - A comprehensive code recently updated. International Journal of Fatigue 2009; 31(1): 50-58, http://dx.doi.org/10.1016/j.ijfatigue.2008.04.002.

27.  ISO 4516. Metallic and other inorganic coatings - Vickers and Knoop microhardness tests. International Organization for Standardization; 1980.

28.  ISO 3057. Non-destructive testing, Metallographic replica techniques of surface examination, International Organization for Standardization, 2011.

29.  Jovančić P, Tanasijević M, Ignjatović D. Relation between numerical model and vibration: Behavior diagnosis for bucket wheel drive assembly at the bucket wheel excavator. Journal of Vibroengineering 2010; 12(4):500-513.

30.  Kowalczyk M, Czmochowski J, Rusiński E. Construction of diagnostic models of the states of developing fault for working parts of the multi-bucket excavator. Eksploatacja i Niezawodnosc- Maintenance and Reliability 2009; 42(2): 17-24

31.  Mellor BG, Rainey RCT, Kirk NE. The static strength of end and T fillet weld connections. Materials & Design 1999; 20(4): 193-205, http://dx.doi.org/10.1016/S0261-3069(99)00027-8.

32.  Milčić D, Miladinović S, Mijajlović M, Marković B. Determination of load spectrum of bucket wheel excavator SRs 1300 in coal strip mine Drmno. Transactions of FAMENA 2013; 37(1): 77-88.

33.  Ognjanović M, Ristić M, Vasin S. BWE traction units failures caused by structural elasticity and gear resonances. Technical Gazette 2013; 20(4): 599-604.

34.  Rusiński E, Czmochowski J, Iluk A, Kowalczyk M. An analysis of the causes of a BWE counterweight boom support fracture. Engineering Failure Analysis 2010; 17(1):179-191, http://dx.doi.org/10.1016/j.engfailanal.2009.06.001.

35.  Rusiński E, Dragan S, Moczko P, Pietrusiak D. Implementation of experimental method of determining modal characteristics of surface mining machinery in the modernization of the excavating unit. Archives of Civil and Mechanical Engineering 2012; 12(4): 471-476, http://dx.doi.org/10.1016/j.acme.2012.07.002.

36. Rusiński E, Czmochowski J, Pietrusiak D. Selected problems in designing and constructing surface mining machinery. FME Transactions 2012; 40(4): 153-164.

37. Rusinski E, Czmochowski J, Pietrusiak D. Problems of steel construction modal models identification. Eksploatacja i Niezawodnosc - Maintenance and Reliability 2012; 14(1): 54-61.

38. Rusiński E, Czmochowski J, Moczko P, Pietrusiak D. Assessment of the correlation between the numerical and experimental dynamic characteristics of the bucket wheel excavator in terms of the operational conditions, FME Transactions 2013; 41(4): 298-304.

39. Rusiński E, Moczko P, Odyjas P, Pietrusiak D. Investigations of structural vibrations problems of high performance machines. FME Transactions 2013; 41(4): 305-310.

40. Shukla AK, Das P, Dutta S, Ray S, Roy H. Failure analysis of a head gear pulley used in coal mines. Engineering Failure Analysis 2013; 31: 48-58, http://dx.doi.org/10.1016/j.engfailanal.2013.01.046.

**Srđan BOŠNJAK**
University of Belgrade
Faculty of Mechanical Engineering
Kraljice Marije 16, 11120 Belgrade 35, Serbia

**Miodrag ARSIĆ**
Institute for Testing of Materials IMS
Bulevar Vojvode Mišića 43, 11000 Belgrade, Serbia

**Sreten SAVIĆEVIĆ**
University of Montenegro
Faculty of Mechanical Engineering
Džordža Vašingtona bb, 81000, Podgorica, Montenegro

**Goran MILOJEVIĆ**
University of Belgrade
Faculty of Mechanical Engineering
Kraljice Marije 16, 11120 Belgrade 35, Serbia

**Dušan ARSIĆ**
University of Kragujevac
Faculty of Engineering
Sestre Janjić 6, 34000 Kragujevac, Serbia

E-mails: sbosnjak@mas.bg.ac.rs, miodrag.arsic@institutims.rs, sreto@ac.me, gmilojevic@mas.bg.ac.rs, dusan.arsic@fink.rs